

## Influence of increasing carbonate saturation in Atlantic bottom water during the late Miocene

Caitlin R. Keating-Bitonti\*, Shanan E. Peters

Department of Geoscience, University of Wisconsin – Madison, Madison, WI 53706, United States of America



### ARTICLE INFO

**Keywords:**  
Thermohaline circulation  
 $\text{CaCO}_3$  preservation  
Stable carbon isotopes  
Macrostratigraphy  
Walvis Ridge  
Carbon cycling

### ABSTRACT

The late Miocene witnessed the tectonic uplift of the Isthmus of Panama, the onset of modern-like thermohaline circulation, changes in global patterns of deep-sea sedimentation, and a negative shift of  $\sim 1\text{\textperthousand}$  in the carbon isotopic composition ( $\delta^{13}\text{C}$ ) of marine carbonate sediments. Although previous work has attributed the late Miocene carbon isotopic shift (LMCS) to biological and environmental factors, the reasons for this apparent shift in the global carbon cycle remain incompletely understood. Here we combine both core-based sedimentological and isotopic data from three Walvis Ridge sites in the southeastern Atlantic Ocean with macrostratigraphic data from the entire Atlantic basin to show that the LMCS marks the establishment of modern, glacial/interglacial seawater carbonate saturation levels in the Atlantic. Between 10 and 7 million years ago (Ma) the Atlantic Ocean shows a trend of increasing seafloor area preserving deep-sea carbonate sediments. Neogene carbonate sedimentation in the Atlantic Ocean peaked at 7 Ma, coinciding with a  $\delta^{13}\text{C}$  shift of approximately  $-0.8\text{\textperthousand}$  in Walvis Ridge benthic foraminifera, similar to the magnitude of LMCS. Northern-sourced waters in the late Miocene likely shifted seawater carbonate chemistry throughout the Atlantic basin by introducing bottom waters with higher carbonate ion concentrations. LMCS reflects the introduction of a carbonate ion effect on North Atlantic Deep Water (NADW) by increasing Northern Hemisphere glacial carbonate weathering. A carbonate ion flux to the Labrador Seawater contribution of NADW raises the possibility of a carbonate burial-mediated feedback with the global climate system that led to additional cooling during the Miocene-Pliocene transition.

### 1. Introduction

Understanding the interactions between ocean circulation, climate, and carbon cycling is central to many questions in the Earth sciences. Deep-sea sediments act as an archive for the evolution of the oceanic and climatic systems (Berger, 1972). The late Miocene carbon isotopic shift (LMCS) initiating  $\sim 7.3$  million years ago (Ma), previously referred to as the Chron 6 carbon shift (Vincent et al., 1980), is an example of an interval when Cenozoic deep-sea sediments preserve a distinct transition in the state of the Earth system. The LMCS represents the last phase in the establishment of the modern, glacial/interglacial carbon cycle, and it is marked by a sustained negative shift of  $\sim 1\text{\textperthousand}$  in the carbon isotopic composition ( $\delta^{13}\text{C}$ ) of marine carbonate sediments (Billups, 2002; Hodell and Kennett, 1986; Keigwin and Shackleton, 1980; Lear et al., 2003; Loutit and Kennett, 1979; Nathan and Leckie, 2009; Vincent et al., 1980). However, the intricacies of the physical and chemical drivers of this isotopic shift and the state of late Miocene climate remain incompletely understood (LaRiviere et al., 2012).

Hypotheses for the global  $\delta^{13}\text{C}$  decrease in the late Miocene include the expansion of  $\text{C}_4$  grasslands (Cerling et al., 1997; Cerling et al., 1993; Quade et al., 1989), a prevalent marine biological bloom (Diester-Haass et al., 2005, 2006) coupled with a transition in the dominance of marine calcareous phytoplankton to siliceous diatoms (Falkowski et al., 2004; Finkel et al., 2005), and an increase in continental silicate weathering (Hodell et al., 1989; Raymo et al., 1988). Although these hypothesized mechanisms could have triggered the LMCS, there is a lack of causal evidence for how they contributed to the global negative isotopic shift and subsequently maintained it over the past 7 million years (Myr).

The transition from the middle to late Miocene is also characterized by intensified mixing of Nordic Sea Overflow Water (NSOW) and Labrador Seawater to form North Atlantic Deep Water (NADW; see Fig. 1), contributing to modern-like North Atlantic meridional overturning circulation (Cramer et al., 2009; Klevenz et al., 2008; Lear et al., 2003; Poore et al., 2006; Thomas and Via, 2007). During this time, the Central American Seaway became constricted with the progressive

\* Corresponding author at: Department of Paleobiology, National Museum of Natural History Smithsonian Institution, Washington, DC 20013-7012, United States of America.

E-mail address: [Keating-Bitonti@si.edu](mailto:Keating-Bitonti@si.edu) (C.R. Keating-Bitonti).

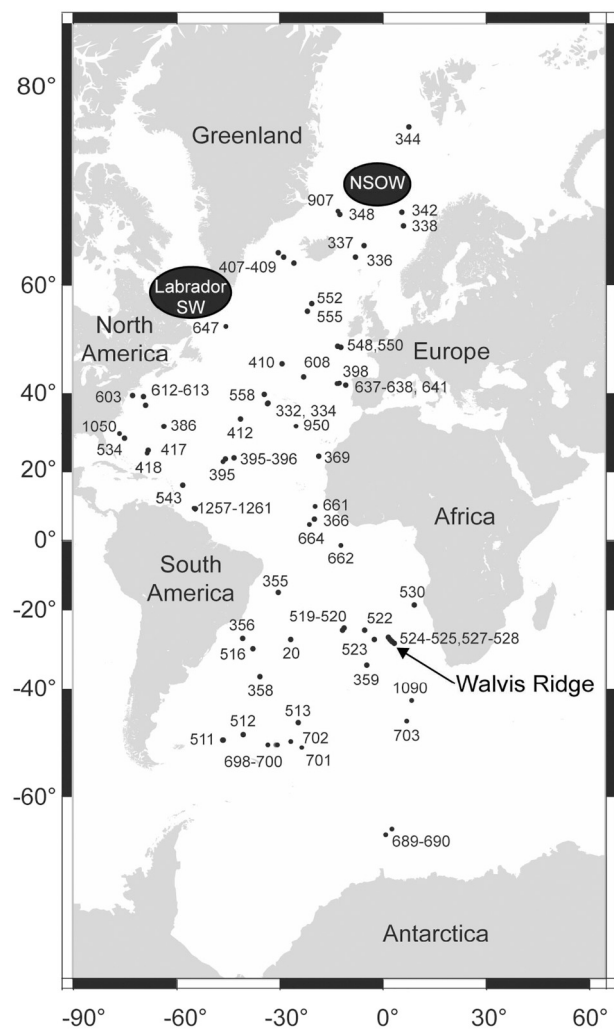


**Fig. 1.** Locations of the 73 Atlantic Deep Sea Drilling Project (DSDP) and Ocean Drilling Program (ODP) sites used to delineate patterns in basin sedimentation. Black ellipses mark the locations of major downwelling in the Northern Hemisphere during the mid to late Neogene (Poore et al., 2006). NADW is composed of both Nordic Seas Overflow Water (NSOW) and Labrador Seawater (SW), contributing to the intensification of North Atlantic meridional overturning circulation (Cramer et al., 2009; de Carvalho Ferreira and Kerr, 2017; Poore et al., 2006). Base map is from the ODP Leg 208 Summary Report (Zachos et al., 2004).

uplift of the Isthmus of Panama (Butzin et al., 2011; Haug and Tiedemann, 1998; Lyle et al., 1995; Nisancioglu et al., 2003; Osborne et al., 2014; Schnitker, 1980; Sepulchre et al., 2014), resulting in distinct shifts in patterns of deep-sea sedimentation associated with the rerouting of deep-water circulation (Delaney and Boyle, 1988; Keller and Barron, 1983; van Andel, 1975). The temporal relationship between shifting global deep-sea sedimentation patterns and evolving bathyal ocean circulation routes during the middle to late Miocene, suggests that LMCS might reflect the chemical and physical transitions of the ocean system. Tectonic events coupled with Northern Hemisphere cooling in the late Miocene likely increased bottom water carbonate ion concentrations throughout the Atlantic basin. Inorganic carbon burial in the Atlantic deep sea association with increased carbonate saturation levels would impose a carbonate ion effect resulting in a negative carbon isotope shift (i.e., LMCS), in addition to a carbonate burial-mediated feedback with the global climate system.

To evaluate the link between the chemical and physical evolution of Atlantic bottom waters during the LMCS, we compiled sedimentological data and analyzed benthic foraminiferal stable carbon isotopic data

from a series of Ocean Drilling Program (ODP) Leg 208 sites drilled along the Walvis Ridge, an aseismic ridge in the southeast Atlantic Ocean (Fig. 1, Zachos et al., 2004). Previous studies identified that Walvis Ridge sediments are sensitive recorders of bottom water conditions associated with deep-sea circulation patterns in the Neogene through present (Bell et al., 2015; Bell et al., 2014; Karas et al., 2017; Klevenz et al., 2008; Thomas and Via, 2007). Here, we integrated newly compiled sedimentological and isotopic Walvis Ridge data with previously published Walvis Ridge fish teeth neodymium isotope records (Thomas and Via, 2007) to trace the sources of these deep waters. We also utilized an Atlantic compilation of deep-sea drilling data to assess basin-scale changes in the extent and type of sedimentation throughout the Neogene. Coupling these basin-wide and local sedimentological data with new and previously compiled Walvis Ridge isotopic data, we test the hypothesis that the introduction of northern-sourced bottom waters to the South Atlantic in the late Miocene increased rates of inorganic carbon burial throughout the Atlantic deep-sea and that the LMCS marks this shift in bottom water carbonate ion concentrations.

## 2. Methods

Sedimentological and geochemical data from ODP Leg 208 on Walvis Ridge (Zachos et al., 2004) allows for the reconstruction of the surrounding water column (e.g., Bell et al., 2015; Bell et al., 2014; Karas et al., 2017) and provides insight into carbon cycling and deep-sea carbonate preservation in the South Atlantic. We analyzed core sediment samples spanning 20 Ma to present from a subset of cores recovered along the Walvis Ridge depth-transsect: Sites 1262, 1266, and 1264 with present-day water depths of 4755, 3798, and 2505 m below sea level (mbsl), respectively. We studied core samples at ~50 cm intervals for Sites 1262 and 1264, and at an interval spacing of ~100 cm for Site 1266.

### 2.1. Age model

Ages assigned to the samples followed the age-depth model of ODP Leg 208 based on shipboard biostratigraphic and magnetostratigraphic data (Zachos et al., 2004) updated to GTS 2012 (Hilgen et al., 2012; Pillans and Gibbard, 2012). We assumed linear sedimentation rates between chronologic tie points to yield a numeric age estimate for each sample. For Site 1264, we applied a 3rd-order polynomial age model calculation from Liebrand et al. (2011) to samples collected from ≥214 m composite depth. The tuned ages from Walvis Ridge Site 1264 reported by Liebrand et al. (2016) generally support previously reported ages from the Walvis Ridge. The lower to upper Miocene sections of Site 1262 are condensed by hiatuses, thereby restricting the age control on samples older than 7 Ma (Zachos et al., 2004). However, previous studies have reported isotopic data reconstructed to be older than 7 Ma from Site 1262 (e.g., Thomas and Via, 2007). Herein we report Neogene sedimentological and isotopic data from Site 1262 recognizing that the ages of samples older than 7 Ma are not well constrained. Instead we used these data to inform the broad physical and chemical patterns of the South Atlantic Ocean prior to and after 7 Ma, but we confidently applying the age model to sediments younger than 7 Ma.

### 2.2. Carbonate sediment records

Here we used coarse fraction weight percent (wt%) data and both shipboard magnetic susceptibility and low-resolution carbonate ( $\text{CaCO}_3$ ) wt% records of Zachos et al. (2004) as proxies to constrain the balance between carbonate export and dissolution in order to reconstruct seawater carbonate saturation in the southeastern Atlantic over the past 20 million years Myr. Relatively high magnetic susceptibility values indicate high terrigenous clay-rich content (Stap et al., 2009) and decreasing values correspond to increasing carbonate

content. We used the shipboard magnetic susceptibility records and  $\text{CaCO}_3$  wt% to track changes in the fine fraction carbonate content (see Lourens et al., 2005; Stap et al., 2009).

Coarse fraction wt% and benthic foraminifera abundance of deep-sea sediment are particularly sensitive to changes in carbonate dissolution (Hancock and Dickens, 2005; Haug and Tiedemann, 1998; Kastanja and Henrich, 2007; Schlanger and Douglas, 1974; Thunell, 1976). We quantified the coarse fraction wt% ( $> 63\text{-}\mu\text{m}$ ) of core samples collected from Sites 1262, 1266, and 1264 to delineate local patterns of carbonate preservation along the Walvis Ridge (Kastanja and Henrich, 2007; Kelly et al., 2010; Lourens et al., 2005; Stap et al., 2009). To determine the coarse fraction wt%, we oven dried the Walvis Ridge core samples at  $32^\circ\text{C}$  for 72 h and then allowed the samples to equilibrate at room temperature for 24 h before taking the mass of each bulk sediment sample. Bulk sediment samples were disaggregated in a mild solution consisting of distilled water and  $\text{H}_2\text{O}_2$  and subsequently washed over a  $63\text{-}\mu\text{m}$  mesh sieve to isolate the coarse fraction. The coarse fraction was then oven dried and weighed again. We calculated the coarse fraction wt% for each sample by dividing the coarse fraction mass by that of the original bulk sediment mass.

### 2.3. Macrostratigraphy

In addition to collecting data that express local changes in carbonate sediment content (i.e., coarse fraction wt%, magnetic susceptibility, and  $\text{CaCO}_3$  wt%), sedimentary data from 73 Atlantic Deep Sea Drilling Project (DSDP) and ODP sites were used to measure patterns of carbonate sedimentation across the Atlantic basin (Fig. 1). We only included sites that were cored continuously from surface sediments to within or near basement rocks. These drill core data were derived from the compilation of Peters et al. (2013), described further in Fraass et al. (2015), and are accessible via the Macrostrat database (Peters et al., 2018). Sedimentological data in the Macrostrat database were compiled from lithostratigraphic descriptions of core material published in the DSDP and ODP Scientific Report volumes (see supplemental Table S4).

The analytical approach of macrostratigraphy (see Hannisdal and Peters, 2010; Peters, 2006) divides the sedimentary record into measurable thicknesses of sediment that were deposited continuously at a specified temporal interval of resolution. In this case, calcareous nanoplankton zones were used to both correlate cores in the Atlantic compilation and to recognize significant hiatuses (Peters et al., 2013). Changes in the spatial distribution and amount of deep-sea sedimentation, and therefore the total number of sedimentary packages, is directly related to changes in ocean circulation, bottom water chemistry, and surface water productivity (Delaney and Boyle, 1988; Keller and Barron, 1983; van Andel, 1975). Macrostratigraphy is a general analytical approach that allows spatial and temporal patterns of sedimentation, and the intervening hiatuses, to be quantified in ways that are closely linked to the processes that govern sedimentation and dissolution in the oceans (Hannisdal and Peters, 2010; Peters et al., 2013), thereby providing a potential proxy record for the proportion of seafloor located above the carbonate compensation depth (CCD).

### 2.4. Benthic isotope analyses

We analyzed benthic foraminifera (*Cibicidoides wuellerstorfi* and *C. mundulus*) picked from sediment samples recovered from Walvis Ridge Sites 1262, 1266, and 1264 for stable carbon isotopes ( $\delta^{13}\text{C}$ ) to constrain both the timing of the LMCS in the southeastern Atlantic and the total magnitude of the isotopic shift among these sites. Stable carbon and oxygen ( $\delta^{18}\text{O}$ ) analyses were made on single specimen benthic foraminifera picked from the  $> 150\text{-}\mu\text{m}$  sieve-size fraction. Stable carbon and oxygen isotope analyses were conducted at the University of Delaware using a GVI IsoPrime dual inlet stable isotope ratio mass spectrometer equipped with a Multiprep sample preparation system. All

benthic foraminifera were sonicated in deionized water to remove fine-grained particles and then oven dried overnight prior to stable isotope analysis. Replicate analyses of the laboratory standards NBS-19 ( $\delta^{13}\text{C} = 1.95\text{\textperthousand}$ ;  $\delta^{18}\text{O} = -2.20\text{\textperthousand}$ ) and an in-house standard (Carrara Marble:  $\delta^{13}\text{C} = 2.25\text{\textperthousand}$ ;  $\delta^{18}\text{O} = -1.27\text{\textperthousand}$ ) yielded an analytical precision of  $0.06\text{\textperthousand}$  for  $\delta^{13}\text{C}$  and  $0.08\text{\textperthousand}$  for  $\delta^{18}\text{O}$  in a size range of 20–200 micrograms. We reported these isotopic values relative to Vienna PeeDee Belemnite (VPDB) using standard  $\delta$  notation.

### 2.5. Statistical analysis

We performed statistical analyses in the statistical computing program R (R Core Team, 2015). To analyze confidence interval differences between the means of benthic foraminiferal  $\delta^{13}\text{C}$  and between the means of fish teeth  $\varepsilon_{\text{Nd}}(t)$  values from Walvis Ridge sites, we applied the Tukey's Honest Significant Difference test using the function *TukeyHSD()*.

## 3. Results

### 3.1. Local and basin-scale patterns of carbonate sedimentation

From 20 to 10 Ma, coarse fraction wt% remained relatively stable at each of the three Walvis Ridge sites (Fig. 2A). Around 10 Ma the coarse fraction wt% increased at Sites 1266 and 1264, followed by a decrease before continuing to increase from  $\sim 7$  Ma to the present. Both Sites 1266 and 1264 recorded low magnetic susceptibility values over the 20 Myr record (Fig. 2C). Site 1262 gradually increased in coarse fraction wt% from  $\sim 7$  Ma to present. However, at Site 1262, proxies for carbonate fine fraction (i.e.,  $\text{CaCO}_3$  wt% and magnetic susceptibility) showed increasing trends of carbonate content that peaked  $\sim 7$  Ma and remained relatively stable to the present (Fig. 2B,C).

Increased carbonate preservation across the Walvis Ridge from 7 Ma onwards (Fig. 2A,B,C) is coeval with an Atlantic basin-wide increase in the total number of sites preserving carbonate sediments (Fig. 2D). Over half of the sites included in the Atlantic macrostratigraphy dataset preserved carbonate sediments during Zone NN11 (8.6–5.6 Ma). Of these sites, the average thickness of carbonate sediments is 45.7 m (Table 1). The modern depths of these sites range from  $\sim 1000$  to 5500 mbsl and we observed no correlation between the water depth of these sites and the thickness of carbonate preserved (Fig. 3), suggesting that increased carbonate preservation was occurring throughout the Atlantic basin (i.e., both at shallow and deep water depths).

### 3.2. Walvis Ridge isotopic records

Prior to 10 Ma, the  $\delta^{13}\text{C}$  values of deep-water site 1262 overlapped with the values of intermediate-water Site 1266 and the shallow-water Site 1264, but diverged from these values by 10 Ma. The  $\delta^{13}\text{C}$  values at sites 1266 and 1264 tracked each other from 10 to 7 Ma and showed a synchronous negative shift that converged on the values of the deep-water Site 1262 by 7 Ma (Fig. 4A), coinciding with the global LMCS (Fig. 4B). Site 1262 had low coarse fraction from 20 to 7 Ma (Fig. 2A) and we recovered few benthic foraminifera in these samples ( $n = 7$ ). Although the ages of these core samples are poorly constrained, we assumed that these foraminifera are not down-slope transport specimens and that their isotopic values represent deep-sea seawater values prior to 7 Ma. The mean  $\delta^{13}\text{C}$  value of the foraminiferal tests collected prior to 7 Ma at the deep-water Site 1262 is  $0.90\text{\textperthousand}$  and following 7 Ma the mean value decreases to  $0.56\text{\textperthousand}$  (Fig. 5A). However, the three oldest recovered benthic foraminifera based on stratigraphic position have a mean  $\delta^{13}\text{C}$  value of  $1.20\text{\textperthousand}$ , suggesting that Site 1262 recorded a trend of decreasing  $\delta^{13}\text{C}$  values over the 20 Myr record (Fig. 4A). Furthermore, the mean  $\delta^{13}\text{C}$  value of the three oldest benthic foraminifera at Site 1262 is similar to the mean  $\delta^{13}\text{C}$  values of Sites 1266 and 1264 prior to 7 Ma,  $1.31\text{\textperthousand}$  and  $1.33\text{\textperthousand}$ , respectively (Fig. 5A).

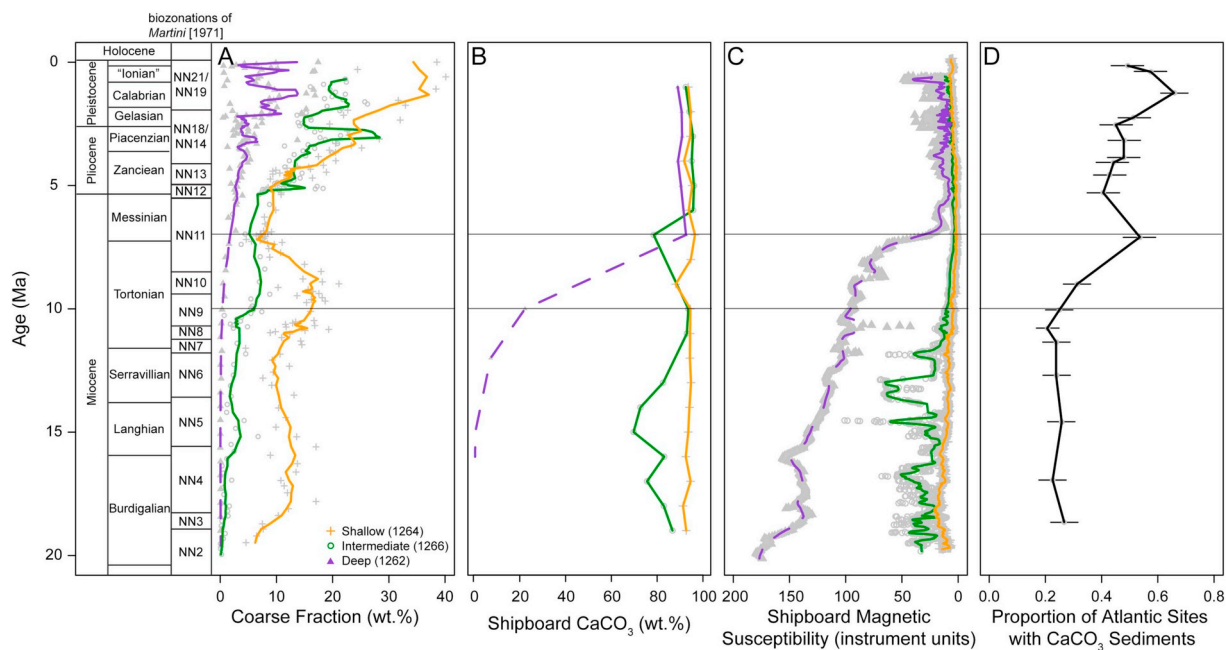


**Fig. 2.** (A) Coarse fraction wt%, (B) shipboard carbonate wt% (Zachos et al., 2004), (C) shipboard magnetic susceptibility (Zachos et al., 2004) for Walvis Ridge Sites 1262 (purple; see Table S1), 1266 (green; see Table S2), and 1264 (orange; see Table S3), and (D) proportion of DSDP and ODP sites with carbonate sediments in the Atlantic Ocean. Macrostratigraphic data are binned into calcareous nannofossil zones and the proportion of the total number of sites of each age that preserve carbonate sediments is plotted at the midpoint of each temporal bin with  $\pm 1$  standard error (see Tables S4). Lines in panel A represent 5-point running averages and the lines in panel C represent 22-point running averages. Horizontal gray lines mark 10 and 7 Ma. Dashed purple lines denote the age model uncertainty for Site 1262 prior to 7 Ma. We plotted Site 1262 data prior to 7 Ma continuing the assumed linear sedimentation rate (Zachos et al., 2004), but herein we make no assertions of an age estimate for these sediments. (For interpretation of the references to colour in this figure legend, the reader is referred to the web version of this article.)

From 20 to 2 Ma, Walvis Ridge Sites 1262 and 1266 generally exhibited parallel trends in  $\delta^{18}\text{O}$  values that diverged  $\sim 2$  Ma when Site 1262 values increased to converge on the  $\delta^{18}\text{O}$  values of Site 1264 (Fig. 4C). The  $\delta^{18}\text{O}$  values of the shallow-water Site 1264 were steadily offset by  $\sim 1.00\text{\textperthousand}$  from Site 1266 over the past 20 Myr. Shallow-water Site 1264 more closely followed the global  $\delta^{18}\text{O}$  record, whereas Sites 1266 and 1262 followed the  $\delta^{18}\text{O}$  record of the South Atlantic (Fig. 4D).

#### 4. Discussion

##### 4.1. Palaeoceanographic change in the Atlantic basin

###### 4.1.1. Evidence for palaeoceanographic change before 10 Ma

Lithostatic plate cooling beneath the Greenland-Scotland Ridge  $\sim 12$  Ma allowed for a greater contribution of NSOW to NADW (Poore et al., 2006). Drift deposits along the Reykjanes Ridge, located south of the Greenland-Scotland Ridge, correlate to intervals of enhanced NADW production beginning in the late Miocene (Wright and Miller, 1993). Inter- and intra-basinal stable carbon and oxygen isotope records show that contributions of NADW varied throughout the middle to late Miocene (Billups, 2002; Flower and Kennett, 1994; Lear et al., 2003; Nathan and Leckie, 2009; Woodruff and Savin, 1989; Wright and Miller, 1993; Wright et al., 1992), but by 12 Ma a north-south gradient in  $\delta^{13}\text{C}$  values in the Atlantic suggests that NADW reached its near-modern flux (Hodell and Venz-Curtis, 2006; Lear et al., 2003; Miller and Fairbanks, 1985; Poore et al., 2006; Woodruff and Savin, 1989; Wright and Miller, 1993; Wright and Miller, 1996; Wright et al., 1991; Wright et al., 1992).

Constriction of the Central America Seaway during the middle Miocene routed NADW away from the eastern Pacific toward the South Atlantic (Coates et al., 2003; Duque-Caro, 1990; Haug and Tiedemann, 1998; Maier-Reimert et al., 1990; Mikolajewicz and Crowley, 1997; Nisancioglu et al., 2003; Sepulchre et al., 2014). The deflection of NADW away from the eastern Pacific, in addition to the coeval

development of a proto-warm pool in the western equatorial Pacific (Nathan and Leckie, 2009), caused the eastern Pacific CCD to shoal. As a result foraminiferal fragmentation increased by 11 Ma (Nathan and Leckie, 2009), marking the eastern Pacific “Carbonate Crash” (Lyle et al., 1995; Pälike et al., 2012; van Andel, 1975; Woodruff and Savin, 1989).

While the eastern Pacific experienced decreasing carbonate saturation levels in the late Miocene, Walvis Ridge showed evidence for an increase in bottom water carbonate saturation levels. Thomas and Via (2007) reported a decline in fish teeth  $\varepsilon_{\text{Nd}}(t)$  values from  $-9.50$  to  $-13.00$  at Site 1262 (Fig. 4E) that spanned  $\sim 13$  to 5 Ma, suggesting that these decreasing values represented bottom waters sourced from the North Atlantic. NADW, a relatively young (less oxidative dissolved CO<sub>2</sub>), carbonate saturated water mass (Nisancioglu et al., 2003; Woodruff and Savin, 1989) would favor deep-sea carbonate preservation. High levels of carbonate preservation at Walvis Ridge Site 1265 (3060 mbsl) point to the increased presence of carbonate saturated bottom water by 10 Ma (Kastanja and Henrich, 2007). Similarly, shipboard CaCO<sub>3</sub> wt% and magnetic susceptibility values at Site 1262 show a trend of increasing preservation of the carbonate fine fraction (Fig. 2; Zachos et al., 2004).

###### 4.1.2. Evidence for palaeoceanographic change between 10 and 7 Ma

On average, Site 1262 sediments have low carbonate content prior to 7 Ma, but by 7 Ma carbonate content at the deep-water site peaked to values similar to the carbonate content of Sites 1266 and 1264. Although the limited age control inhibits our ability to identify the time at which this shift to increasing carbonate preservation at Site 1262 began, it likely took place between 10 and 7 Ma and was driven by increasing carbonate saturation levels in Atlantic deep waters.

The Atlantic Ocean basin first experienced an increasing number of sites preserving carbonate sediments  $\sim 10$  Ma (i.e., the area of seafloor preserving deep-sea carbonate sediments; see Fig. 2D). This initial rise occurred approximately 3 Myr prior to the maximum extent of seafloor

**Table 1**

Thickness of carbonate sediments preserved in Atlantic DSDP and ODP sites during calcareous nannofossil Zone NN11 (8.6–5.6 Ma). Site depth is present-day water depth (echo-sounding) reported in the *Scientific Report* volumes.

Site	Hole	Depth (mbsl)	Number of units	Thickness (m)
DSDP	334	334	2619	2
DSDP	359	C	1658	1
DSDP	366	CO	2853	1
DSDP	369	CO	1752	1
DSDP	395	1	4484	2
DSDP	398	CO	3910	1
DSDP	407	407	2472	2
DSDP	408	40	1624	1
DSDP	410	41	2975	2
DSDP	516	F	1313	1
DSDP	519	519	3769	1
DSDP	521	521	4125	2
DSDP	523	1	4565	1
DSDP	525	CO	2467	1
DSDP	527	1	4428	2
DSDP	528	CO	3800	1
DSDP	530	A	4629	4
DSDP	534	CO	4973	1
DSDP	548	CO	1251	2
DSDP	550	CO	4420	1
DSDP	552	CO	2301	2
DSDP	555	555	1659	3
DSDP	558	CO	3754	1
DSDP	603	CO	4633	2
DSDP	608	608	3526	1
ODP	637	A	5307	5
ODP	638	CO	4661	2
ODP	647	A	3862	1
ODP	661	A	4006	2
ODP	664	D	3806	1
ODP	689	B	2080	2
ODP	690	C	2914	1
ODP	701	C	4637	1
ODP	702	B	3083	2
ODP	950	A	5438	9
ODP	1258	CO	3192	1
ODP	1261	CO	1899	1
Mean			45.7	

**Table 2**

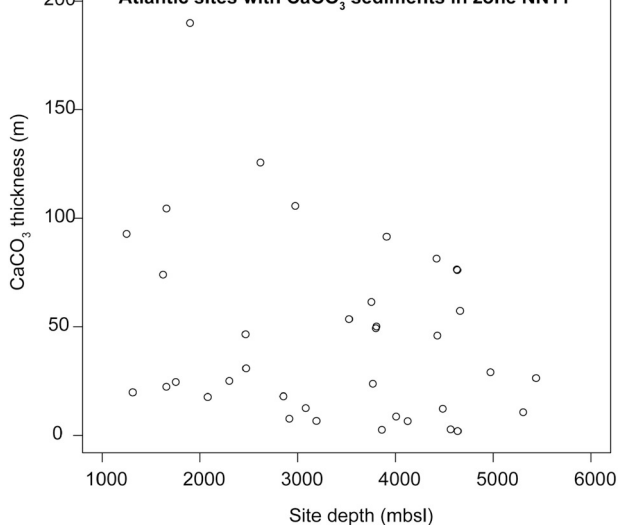
Reported *p*-values from Tukey's tests comparing the median (a) benthic foraminiferal  $\delta^{13}\text{C}$  (this study) and (b) fish teeth  $\varepsilon_{\text{Nd}}(t)$  value (Via and Thomas, 2006) of Walvis Ridge Sites 1262, 1266, and 1264 prior to and following 7 Ma. Note there are no  $\varepsilon_{\text{Nd}}(t)$  data for Site 1266. Asterisks denote a statistically significant difference ( $p$ -value < 0.05).

#### A. Comparison statistics for carbon isotopes

$\delta^{13}\text{C}$	1262		1266		1264	
	$\geq 7$ Ma	< 7 Ma	$\geq 7$ Ma	< 7 Ma	$\geq 7$ Ma	< 7 Ma
1262	$\geq 7$ Ma	NA	0.027*	0.012*	0.488	0.004*
	< 7 Ma	NA	< 0.001*	0.033*	< 0.001*	< 0.001*
1266	$\geq 7$ Ma		NA	< 0.001*	0.999	< 0.001*
	< 7 Ma		NA	< 0.001*	0.245	
1264	$\geq 7$ Ma			NA	< 0.001*	
	< 7 Ma			NA		

#### B. Comparison statistics for neodymium isotopes

$\varepsilon_{\text{Nd}}(t)$	1262		1264	
	$\geq 7$ Ma	< 7 Ma	$\geq 7$ Ma	< 7 Ma
1262	$\geq 7$ Ma	NA	< 0.001*	0.981
	< 7 Ma	NA	< 0.001*	0.178
1264	$\geq 7$ Ma		NA	0.981
	< 7 Ma		NA	

**Fig. 3. Atlantic sites with  $\text{CaCO}_3$  sediments in zone NN11**

**Fig. 3.** Depth to sea floor (mbsl, meters below sea level) of Atlantic DSDP and ODP sites preserving carbonate during Zone NN11 (8.6–5.6 Ma) and the corresponding thicknesses of  $\text{CaCO}_3$  sediments (see Table 1). There is no correlation between modern site water depth and the thickness of carbonate sediments in Zone NN11 ( $p > 0.1$  and  $R^2 = 0.05$ ).

blanketed in carbonate sediments in the Neogene (~7 Ma). The increase in carbonate saturation of Atlantic bottom waters (Fig. 2D) followed the “Carbonate Crash” in the Caribbean and along the Ceara Rise (Nathan and Leckie, 2009; Roth et al., 2000), supporting a rerouting of Atlantic bottom water circulation patterns associated with the constriction of the Central American Seaway.

Neodymium isotope data suggest that the shift in carbonate chemistry at Walvis Ridge was causally linked to changing source waters in the southeastern Atlantic during the late Miocene (Via and Thomas, 2006). Variations in Walvis Ridge fish teeth  $\varepsilon_{\text{Nd}}(t)$  records are contemporaneous with the shifts observed in both our Walvis Ridge sedimentological and  $\delta^{13}\text{C}$  records (Figs. 2 and 4). A decrease in fish teeth  $\varepsilon_{\text{Nd}}(t)$  values at Site 1262 from 13 to 5 Ma (Fig. 4E), suggests that the deeper portion of the southeastern Atlantic water column was bathed by a water mass comprised of a mixture of NSOW and Labrador Seawater, forming NADW (see Fig. 1; Thomas and Via, 2007). Decreasing carbon isotopic values at Site 1262 between 10 and 7 Ma (Fig. 4) are coeval with a trend of increasing carbonate content at this deep water site (Fig. 2) and are bracketed by decreasing  $\varepsilon_{\text{Nd}}(t)$  values (Fig. 4E). Thus, we interpret the temporal offset between the negative  $\delta^{13}\text{C}$  shifts at Site 1262 and Sites 1266 and 1264 to suggest that the northern-sourced waters first intersected Walvis Ridge ~10 Ma and gradually changed the carbon chemistry of its water column over the span of 3 Myr (Fig. 4A).

#### 4.1.3. Evidence for palaeoceanographic change after 7 Ma

By ~7 Ma, significant deep-water exchange with the Pacific Ocean had ceased (Osborne et al., 2014). As a consequence, the South Atlantic seafloor became bathed in NADW, thereby enhancing carbonate preservation in the deep-sea with the suppression of the lysocline and CCD (see Moore et al., 1978; van Andel, 1975; Zachos et al., 2004). Walvis Ridge isotopic and sedimentologic data, in addition to the Atlantic macrostratigraphic records, suggest that bottom waters with relatively high carbonate saturation levels were pervasive throughout the Atlantic Ocean basin by 7 Ma. Site 1262 carbonate content remained both stable and high from 7 Ma to the present, signaling a permanent shift in the carbonate saturation level of Atlantic bottom waters.

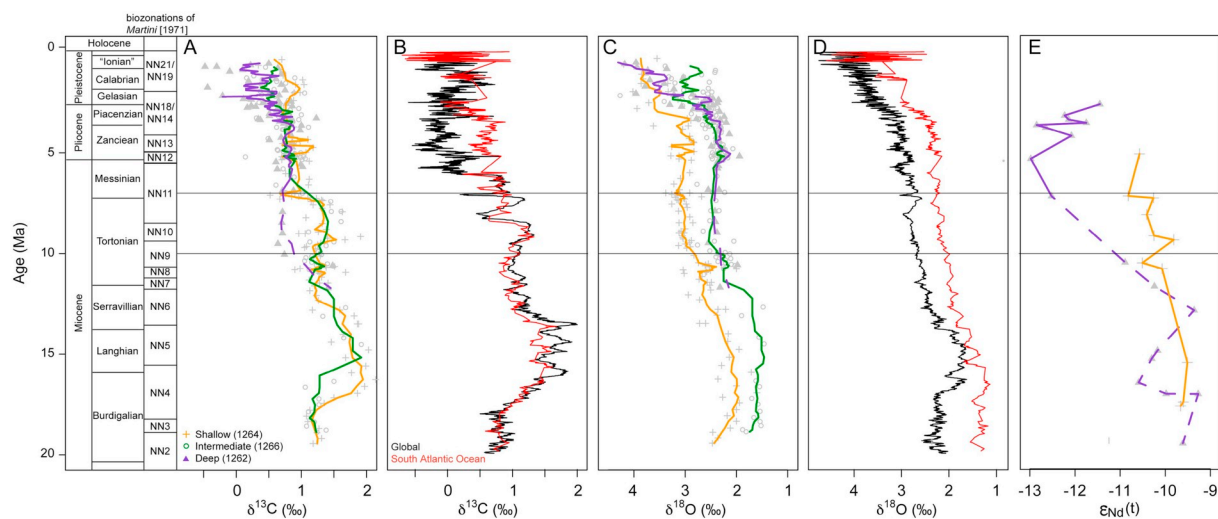


**Fig. 4.** (A) New stable carbon isotope data for Walvis Ridge Sites 1262 (purple; see Table S1), 1266 (green; see Table S2), and 1264 (orange; see Table S3); (B) global (black) and Atlantic Ocean (red) benthic foraminiferal stable carbon isotope data; (C) new oxygen isotope records for Walvis Ridge Sites 1262, 1266, and 1264; (D) global marine and Atlantic Ocean benthic foraminiferal oxygen isotope data; and (E) previously published neodymium isotope data from Walvis Ridge Sites 1262 and 1264 (Thomas and Via, 2007). In panels A and C, purple, green, and orange lines representing 5-point running averages. In Panels B and D, red and black lines represent 22-point running averages of the South Atlantic stable isotopic data compiled by Cramer et al. (2009) and the global compilation (Zachos et al., 2008), respectively. Horizontal gray lines mark 10 and 7 Ma. Dashed purple lines in panels A, C, and E, denote the age model uncertainty for Site 1262 prior to 7 Ma. We plotted Site 1262 data prior to 7 Ma continuing the assumed linear sedimentation rate (Zachos et al., 2004), but herein we make no assertions of an age estimate for these sediments. (For interpretation of the references to colour in this figure legend, the reader is referred to the web version of this article.)

#### 4.2. Northern Hemisphere glaciation

Warm, salty surface waters delivered to the North Atlantic via the Gulf Stream with the constriction of the Central American Seaway (Burton et al., 1997; Haug and Tiedemann, 1998; Keigwin, 1982) enhanced the moisture budget in the Northern Hemisphere and likely promoted the growth of sea and continental ice (Lunt et al., 2008). Although modeling studies based on deep-sea benthic isotope records suggest stable sea levels through the Neogene and limited Northern Hemisphere glaciation prior to 5 Ma (de Boer et al., 2010; de Boer et al., 2012; Stap et al., 2017), benthic foraminiferal Mg/Ca and  $\delta^{18}\text{O}$  data (Billups and Schrag, 2003; Lear et al., 2003; Schnitker, 1980; Shackleton and Kennett, 1975; Shevenell et al., 2004; Wright and Miller, 1996; Wright et al., 1992), in addition to alkenone-based records (Herbert et al., 2016), from the middle to late Miocene provide indirect

evidence for both climate cooling and increasing ice volume in both hemispheres. Occurrences of ice rafted debris in the North Atlantic, North Pacific, and Arctic Ocean provides direct evidence for the presence of Northern Hemisphere continental ice in the middle Miocene that intensified through the late Miocene (Fronval and Jansen, 1996; Krissek, 1995; Larson et al., 1994; Wolf-Welling et al., 1996). A biomarker palaeo-sea-ice proxy provides evidence for high latitude seasonal sea-ice coverage and a general cooling trend in the Northern Hemisphere from ~12 to 5 Ma (Stein et al., 2016).

Northern Hemisphere glaciation in the late Miocene and early Pliocene likely did not intensify the production of NADW formation (Bell et al., 2015; Frank et al., 2002), but instead influenced the carbonate chemistry of this water mass. Evidence for the existence of continental ice sheet growth during the late Miocene in the Northern Hemisphere (e.g., Billups and Schrag, 2003; Flower and Kennett, 1995;

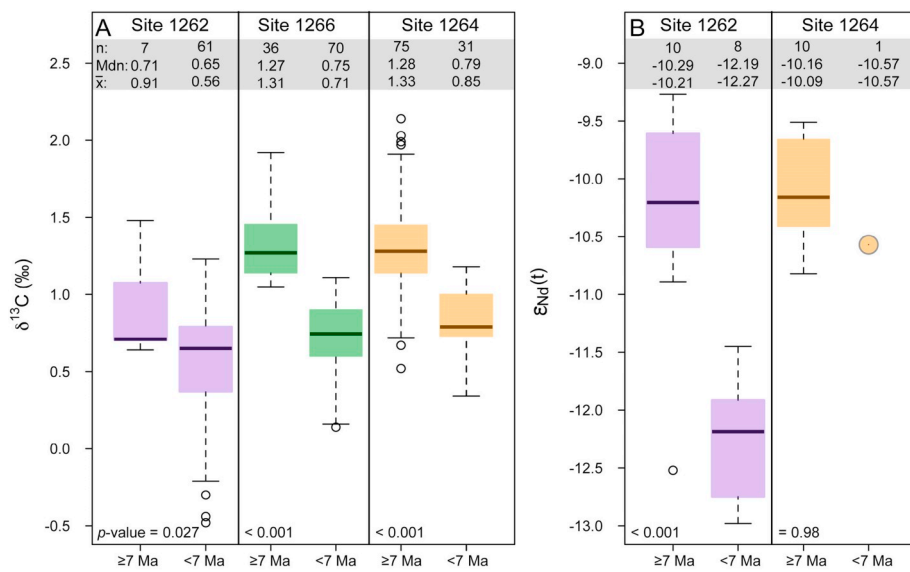


**Fig. 5.** Boxplots depicting the isotopic shifts at 7 Ma in (A) our Walvis Ridge carbon isotope data from Sites 1262 (purple), 1266 (green), and 1264 (orange) and (B) the Walvis Ridge fish teeth neodymium isotope data from Sites 1262 and 1264 analyzed by Thomas and Via (2007). Whiskers represent the minimum and maximum of data within 1.5 times the interquartile range of the median. We report the sample size (n), median (Mdn), and mean ( $\bar{x}$ ) for each boxplot in the upper gray band. Each site exhibits a statistically significant lower  $\delta^{13}\text{C}$  values following 7 Ma ( $p$ -value < 0.05). Note that  $\delta^{13}\text{C}$  values are similar prior to their negative shifts and then overlap following their shifts. Although neodymium isotope records from Walvis Ridge are sparse, we observe a similar pattern at Site 1262 (Table 2). The negative  $\delta^{13}\text{C}$  shift likely occurred prior to 7 Ma for Site 1262, but our limited age control at this site does not allow for an accurate age estimate for when this shift occurred. The mean and median  $\delta^{13}\text{C}$  values of the three oldest foraminiferal specimens from Site 1262 are 1.21‰ and 1.41‰, respectively, more closely aligning with the  $\geq 7$  Ma  $\delta^{13}\text{C}$  values of Site 1266 and 1264 (see Fig. 4A). (For interpretation of the references to colour in this figure legend, the reader is referred to the web version of this article.)

Krissek, 1995; Larson et al., 1994; Wolf-Welling et al., 1996) likely increased physical weathering of continental material. Approximately 25% (~4,900,000 km<sup>2</sup>) of the presently exposed continents north of 60°N have surface bedrock composed of carbonate-bearing sedimentary deposits (Harrison et al., 2011). A 30 to 100 m fall in sea level (Haq et al., 1987; Miller et al., 2005), associated with ice growth on Antarctica during the middle to late Miocene (Flower and Kennett, 1994, 1995; Naish et al., 2009; Schnitker, 1980; Shackleton and Kennett, 1975; Shevenell et al., 2004), likely increased the area of exposed continental shelves, much of which is blanketed by carbonate-bearing sedimentary deposits (Opdyke and Walker, 1992; Opdyke and Wilkinson, 1988). Increased flux of carbonate ions to the North Atlantic would have influenced the saturation level of NADW and enhanced carbonate preservation throughout the Atlantic basin (Fig. 2D; see Tables S1 and S2). The weathering of carbonate sediments, unlike silicate minerals, supplied carbonate ions to the ocean with no net effect on atmospheric  $p\text{CO}_2$  (Lea et al., 1999).

Laboratory experiments demonstrated that  $\delta^{13}\text{C}$  values in both planktic and benthic foraminiferal tests decreased as the carbonate ion concentration of the cultured reservoir increased (McCorkle et al., 2008; Spero et al., 1997). The  $\text{CO}_3^{2-}$  concentration change required to decrease the  $\delta^{13}\text{C}$  values of Walvis Ridge benthic foraminiferal tests during the LMCS can be calculated using an empirical relationship between carbonate ion concentration ( $\mu\text{mol/kg}$ ) and test  $\delta^{13}\text{C}$  (%) (Spero et al., 1997):

$$\delta^{13}\text{C} = 1.90 - 0.012 [\text{CO}_3^{2-}] \quad (1)$$

Assuming that the increased carbonate ion concentration of Atlantic bottom water was the only factor driving the LMCS, an approximately 0.80‰ decrease in  $\delta^{13}\text{C}$  requires an increase of  $\sim 9.0 \times 10^{16}$  mol of  $\text{CO}_3^{2-}$  in the global ocean, or ~1% the present-day global carbonate ion supply ( $\sim 7.8 \times 10^{18}$  mol) (Kump and Arthur, 1999). Although, modern NADW has a  $\delta^{13}\text{C}$  signature of ~1.00‰ (Woodruff and Savin, 1989; Wright and Miller, 1993), we do not interpret the negative  $\delta^{13}\text{C}$  shift recorded at Walvis Ridge to represent a decreased presence of North Atlantic meridional overturning circulation, the traditional interpretation of modern, marine carbon isotope values (e.g., Bell et al., 2015; Bell et al., 2014). Instead, we propose that NADW, a young, well-oxygenated water mass carrying a Northern Hemisphere continent-derived  $\text{CO}_3^{2-}$  signal, imposed a carbonate ion effect on benthic foraminiferal tests (Tedford and Kelly, 2004) at the LMCS. This benthic foraminiferal carbonate ion effect had a twofold effect. First, it decreased  $\delta^{13}\text{C}$  values at Walvis Ridge with the initial introduction of NADW to the South Atlantic and, second, promoted both local and basin-wide changes in the pattern of deep-sea carbonate sedimentation and preservation between 10 and 7 Ma.

## 5. Conclusion

We attribute the LMCS and the subsequent stability of the deep-sea carbon isotope record over the past 7 Myr to the formation and establishment of NADW in the late Miocene. The initial build-up of continental ice in the Northern Hemisphere, due to increased moisture derived from the redirected Gulf Stream, increased the physical weathering of continental crustal rocks and carbonate-bearing sedimentary cover, thereby delivering an increased flux of carbonate ions to the source areas of NADW (i.e., Norwegian-Greenland Sea and Labrador Sea). This increase in carbonate saturation in northern-sourced deep waters imposed both a carbonate ion effect on benthic foraminifera and suppressed the lysocline and CCD, enhancing carbonate preservation in the deep Atlantic starting by ~10 Ma. By the end of the Miocene the intensification of these northern-sourced deep waters grew throughout the entire Atlantic Ocean basin and have since persisted to the present, ultimately contributing to the establishment of the modern global carbon cycle. Although multiple hypotheses have been proposed for the LMCS, a carbonate ion effect associated with the establishment of

NADW in the late Miocene, the modern global deep-sea water conveyor system, explains the global and permanent negative carbon isotope shift that has maintained to the present.

## Acknowledgements

This work was supported by a grant from the Geological Society of America, and graduate student research fellowships awarded by ConocoPhillips and the National Science Foundation Graduate Research Fellowship Program to C. R. Keating-Bitonti. This research used samples provided by the Integrated Ocean Drilling Program. We are grateful to Appy Sluijs and Ellen Thomas for their constructive feedback and for the comments from two anonymous reviewers that also helped to improve the manuscript. We thank Bruce H. Wilkinson, Noel A. Heim, and Stephen R. Meyers for helpful discussion. D. Clay Kelly provided invaluable guidance and discussion throughout this work. We thank Katharina Billups at the University of Delaware for running stable isotope analyses.

## Appendix A. Supplementary data

Supplementary data to this article can be found online at <https://doi.org/10.1016/j.palaeo.2019.01.006>.

## References

- Bell, D.B., Jung, S.J.A., Kroon, D., Lourens, L.J., Hodell, D.A., 2014. Local and regional trends in Plio-Pleistocene  $d^{18}\text{O}$  records from benthic foraminifera. *Geochem. Geophys. Geosyst.* 15, 3304–3321.
- Bell, D.B., Jung, S.J.A., Kroon, D., Hodell, D.A., Lourens, L.J., Raymo, M.E., 2015. Atlantic deep-water response to the early Pliocene shoaling of the Central American Seaway. *Sci. Rep.* 5, 1–11.
- Berger, W.H., 1972. Deep sea carboantes: dissolution facies and age depth constancy. *Nature* 236, 392–395.
- Billups, K., 2002. Late Miocene through early Pliocene deep water circulation and climate changed viewed from the sub-Antarctic South Atlantic. *Palaeogeogr. Palaeoclimatol. Palaeoecol.* 185, 287–307.
- Billups, K., Schrag, D., 2003. Application of benthic foraminiferal Mg/Ca ratios to questions of Cenozoic climate change. *Earth Planet. Sci. Lett.* 209, 181–195.
- Burton, K.W., Ling, H.-F., O'Nions, K., 1997. Closure of the Central American Isthmus and its effect on deep-water formation in the North Atlantic. *Nature* 386, 382–385.
- Butzin, M., Lohmann, G., Bickert, T., 2011. Miocene ocean circulation inferred from marine carbon cycle modeling combined with benthic isotope records. *Paleoceanography* 26, PA1203.
- Cerling, T.E., Wang, Y., Quade, J., 1993. Expansion of C4 ecosystems as an indicator of global ecological change in the late Miocene. *Nature* 361, 344–345.
- Cerling, T.E., Harris, J.M., MacFadden, B.J., Leakey, M.G., Quade, J., Eisenmann, V., Ehleringer, J.R., 1997. Global vegetation change through the Miocene/Pliocene boundary. *Nature* 389, 153–158.
- Coates, A.G., Aubry, M.-P., Berggren, W.A., Collins, L.S., Kunk, M., 2003. Early Neogene history of the Central American arc from Bocas del Toro, western Panama. *GSA Bull.* 115, 271–287.
- Cramer, B.S., Toggweiler, J.R., Wright, J.D., Katz, M.E., Miller, K.G., 2009. Ocean overturning since the Late Cretaceous: inferences from new benthic foraminiferal isotope compilation. *Paleoceanography* 24, PA4216.
- de Boer, B., van de Wal, R.S.W., Bintanja, R., Lourens, L.J., Tuenter, E., 2010. Cenozoic global ice-volume and temperature simulations with 1-D ice-sheet models forced by benthic  $d^{18}\text{O}$  records. *Ann. Glaciol.* 55, 23–33.
- de Boer, B., van de Wal, R.S.W., Lourens, L.J., Bintanja, R., 2012. Transient nature of the Earth's climate and the implications for the interpretation of benthic  $d^{18}\text{O}$  records. *Palaeogeogr. Palaeoclimatol. Palaeoecol.* 335–336, 4–11.
- de Carvalho Ferreira, M.L., Kerr, R., 2017. Source water distribution and quantification of north atlantic deep water and antarctic bottom water in the atlantic ocean. *Prog. Oceanogr.* 153, 66–83.
- Delaney, M.L., Boyle, E.A., 1988. Tertiary Paleoeceanic chemical variability: unintended consequences of simple geochemical models. *Paleoceanography* 3, 137–156.
- Diester-Haass, L., Billups, K., Emeis, K., 2005. In search of the late Miocene-early Pliocene “biogenic bloom” in the Atlantic Ocean (Ocean Drilling Program Sites 982, 925, and 1088). *Paleoceanography* 20, PA4001.
- Diester-Haass, L., Billups, K., Emeis, K., 2006. Late Miocene carbon isotope records and marine biological productivity: was there a (dusty) link? *Paleoceanography* 21, PA4216.
- Duque-Caro, H., 1990. Neogene stratigraphy, paleoceanography and paleobiology in northwest South America and the evolution of the Panama Seaway. *Palaeogeogr. Palaeoclimatol. Palaeoecol.* 77, 203–234.
- Falkowski, P., Katz, M.E., Knoll, A., Quigg, A., Raven, J., Schofield, O., Taylor, F.J.R., 2004. The evolution of modern eukaryotic phytoplankton. *Science* 305, 354–360.
- Finkel, Z., Katz, M.E., Wright, J.D., Schofield, O., Falkowski, P., 2005. Climatically driven

- macroevolutionary patterns in the size of marine diatoms over the Cenozoic. *Proc. Natl. Acad. Sci.* 102, 8927–8932.
- Flower, B.P., Kennett, J.P., 1994. The middle Miocene climatic transition; East Antarctic ice sheet development, deep ocean circulation and global carbon cycling. *Palaeogeogr. Palaeoclimatol. Palaeoecol.* 108, 537–555.
- Flower, B.P., Kennett, J.P., 1995. Middle Miocene deepwater paleoceanography in the southwest Pacific: relations with East Antarctic ice sheet development. *Paleoceanography* 10, 1095–1112.
- Fraass, A.J., Kelly, D.C., Peters, S.E., 2015. Macroevolutionary history of the planktic foraminifera. *Annu. Rev. Earth Planet. Sci.* 43, 139–166.
- Frank, M., Whiteley, N., Kasten, S., Hein, J.R., 2002. North Atlantic deep water export to the Southern Ocean over the past 14 Myr: evidence from Nd and Pb isotopes in ferromanganese crusts. *Paleoceanography* 17, 1022.
- Fronval, T., Jansen, E., 1996. Late Neogene paleoclimates and paleoceanography in the Iceland-Norwegian Sea: evidence from the Iceland and Voring Plateaus. In: Thiede, J., Myhre, A.M., Firth, J.V., Johnson, G.L., Ruddiman, W.F. (Eds.), *Proceedings of the Ocean Drilling Program, Scientific Results*, College Station, pp. 455–468.
- Hancock, H.J.L., Dickens, G.R., 2005. Carbonate dissolution episodes in Paleocene and Eocene sediment, Shatsky Rise, west-central Pacific. In: Blaer, T.J., Premoli Silva, I., Malone, M.J. (Eds.), *Proceedings of the Ocean Drilling Program Initial Reports*, College Station, TX.
- Hannisdal, B., Peters, S.E., 2010. On the relationship between macrostratigraphy and geological processes: quantitative information capture and sampling robustness. *J. Geol.* 118, 111–130.
- Haq, B.U., Hardenbol, J., Vail, P.R., 1987. Chronology of fluctuating sea levels since the Triassic. *Science* 235, 1156–1167.
- Harrison, J.C., St-Onge, M.R., Petrov, O.V., Strelnikov, S.I., Lopatin, B.G., Wilson, F.H., Tella, S., Paul, D., Lynds, T., Shokalsky, S.P., Hults, C.K., Bergman, S., Jepsen, H.F., Solli, A., 2011. In: Canada, G.S.O. (Ed.), *Geologic Map of the Arctic*, 2159A ed. "A" Series Map Natural Resources Canada.
- Haug, G.H., Tiedemann, R., 1998. Effect of the formation of the Isthmus of Panama on Atlantic Ocean thermohaline circulation. *Nature* 393, 673–676.
- Herbert, T.D., Lawrence, K.T., Tzanova, A., Cleaveland Peterson, L., Caballero-Gill, R., Kelly, C.S., 2016. Late Miocene global cooling and the rise of modern ecosystems. *Nat. Geosci.* 9, 843–847.
- Hilgen, F.J., Lourens, L.J., van Dam, J.A., 2012. The Neogene period. Elsevier.
- Hodell, D.A., Kennett, J.P., 1986. Late Miocene - early Pliocene stratigraphy and paleoceanography of the South Atlantic and southwest Pacific Oceans: a synthesis. *Paleoceanography* 1, 285–311.
- Hodell, D.A., Venz-Curtis, K.A., 2006. Late Neogene history of deepwater ventilation in the Southern Ocean. *Geochem. Geophys. Geosyst.* 7, Q09001.
- Hodell, D.A., Mueller, P.A., McKenzie, J.A., Mead, G.A., 1989. Strontium isotope stratigraphy and geochemistry of the late Neogene ocean. *Earth Planet. Sci. Lett.* 92, 165–178.
- Karas, C., Nürnberg, D., Bahr, A., Groeneveld, J., Herrle, J.O., Tiedemann, R., deMenocal, P.B., 2017. Pliocene oceanic seaways and global climate. *Sci. Rep.* 7, 1–7.
- Kastanja, M.M., Henrich, R., 2007. Grain-size variations in pelagic carbonate oozes from the Walvis Ridge - SE Atlantic Ocean (ODP Site 1265): a low resolution Miocene record of carbonate sedimentation and preservation. *Mar. Geol.* 237, 97–108.
- Keigwin, L., 1982. Isotopic paleo-oceanography of the Caribbean and East Pacific - role of Panama uplift in late Neogene time. *Science* 217, 350–352.
- Keigwin, L.D., Shackleton, N.J., 1980. Uppermost Miocene carbon isotope stratigraphy of a piston core in the equatorial Pacific. *Nature* 284, 613–614.
- Keller, G., Barron, J.A., 1983. Paleoceanographic implications of Miocene deep-sea hiatuses. *Geol. Soc. Am. Bull.* 94, 590–613.
- Kelly, D.C., Nielsen, T.M.J., McCarren, H.K., Zachos, J.C., Röhl, U., 2010. Spatiotemporal patterns of carbonate sedimentation in the South Atlantic: implications for carbon cycling during the Paleocene-Eocene thermal maximum. *Palaeogeogr. Palaeoclimatol. Palaeoecol.* 293, 30–40.
- Klevven, V., Vance, D., Schmidt, D.N., Mezger, K., 2008. Neodymium isotopes in benthic foraminifera: core-top systematics and a down-core record from the Neogene south Atlantic. *Earth Planet. Sci. Lett.* 265, 571–587.
- Krissek, L.A., Rae, D.K., Basov, J.A., Scholl, D.W., Allan, J.F., 1995. Late Cenozoic ice-raftering records from Leg 145 sites in the North Pacific: Late Miocene onset Late Pliocene intensification and Plio-Pleistocene events. In: *Proceedings from the Ocean Drilling Program, Scientific Results*, College Station, pp. 179–194.
- Kump, L.R., Arthur, M.A., 1999. Interpreting carbon-isotope excursions: carbonates and organic matter. *Chem. Geol.* 161, 181–198.
- LaRiviere, J., Ravelo, A.C., Crimmins, A., Dekens, P.S., Ford, H.L., Lyle, M., Wara, M.W., 2012. Late Miocene decoupling of oceanic warmth and atmospheric carbon dioxide forcing. *Nature* 486, 97–100.
- Larson, H.C., Saunders, A.D., Clift, P.D., Begét, J., Spezzaferri, S., Ali, J., Cambray, H., Demant, A., Fitton, G., Fram, M.S., Fukuma, K., Gieskes, J., Holmes, M.A., Hunt, J., Lacasse, C., Larsen, L.M., Lykke-Anderson, H., Meltsner, A., Morrison, M.L., Nemoto, N., Okay, N., Saito, S., Sinton, C., Stax, R., Vallier, T.L., Vandamme, D., Werner, R., 1994. Seven million years of glaciation in Greenland. *Science* 264, 952–955.
- Lea, D., Bijma, J., Spero, H.J., Archer, D., 1999. Implications of a carbonate ion effect on shell carbon and oxygen isotopes for glacial ocean conditions. In: Fischer, G., Wefer, G. (Eds.), *Use of Proxies in Paleoceanography: Examples from the South Atlantic*. Springer, Berlin, Heidelberg, pp. 513–522.
- Lear, C.H., Rosenthal, Y., Wright, J.D., 2003. The closing of a seaway: ocean water masses and global climate change. *Earth Planet. Sci. Lett.* 210, 425–436.
- Liebrand, D., Lourens, L.J., Hodell, D.A., de Boer, B., van de Wal, R.S.W., Pälike, H., 2011. Antarctic ice sheet and oceanographic response to eccentricity forcing during the early Miocene. *Clim. Past* 7, 869–880.
- Liebrand, D., Beddow, H.M., Lourens, L.J., Pälike, H., Raffi, I., Bohaty, S.M., Hilgen, F.J., Saes, M.J.M., Wilson, P.A., van Dijk, A.E., Hodell, D.A., Kroon, D., Huck, C.E., Batenburg, S.J., 2016. Cyclostratigraphy and eccentricity tuning of the early Oligocene through early Miocene (30.1–17.1 Ma): *Cibicides mundulus* stable oxygen and carbon isotope records from Walvis Ridge Site 1264. *Earth Planet. Sci. Lett.* 450, 392–405.
- Lourens, L.J., Sluijs, A., Kroon, D., Zachos, J.C., Thomas, E., Röhl, U., Bowles, J., Raffi, I., 2005. Astronomical pacing of late Paleocene to early eocene global warming events. *Nature* 435, 1083–1087.
- Loutit, T.S., Kennett, J.P., 1979. Application of carbon isotope stratigraphy to late Miocene shallow marine sediments, New Zealand. *Science* 204, 1196–1199.
- Lunt, D.J., Valdes, P.J., Haywood, A., Rutt, I.C., 2008. Closure of the Panama Seaway during the Pliocene: implications for climate and Northern Hemisphere glaciation. *Clim. Dyn.* 30, 1–18.
- Lyle, M., Dadey, K.A., Farrell, J.W., 1995. The late Miocene (11–8 Ma) eastern Pacific carbonate crash: evidence for reorganization of deep-water circulation by the closure of the Panama gateway. *Proc. ODP Sci. Results* 138, 821–838.
- Maier-Reimer, E., Mikolajewicz, U., Crowley, T., 1990. Ocean general circulation model sensitivity experiment with an open Central American Isthmus. *Paleoceanography* 5, 349–366.
- McCorkle, D.C., Bernhard, J.M., Hintz, C.J., Blanks, J.K., Chandler, G.T., Shaw, T.J., 2008. The carbon and oxygen stable isotopic composition of cultured benthic foraminifera. In: Austin, W.E.N., James, R.H. (Eds.), *Biogeochemical controls on paleoceanographic environmental proxies*. Geological Society, London, pp. 135–154.
- Mikolajewicz, U., Crowley, T., 1997. Response of a coupled ocean/energy balance model to restricted flow through the Central American Isthmus. *Paleoceanography* 12, 429–441.
- Miller, K.G., Fairbanks, R.G., 1985. Oligocene to Miocene carbon isotope cycles and abyssal circulation changes. In: Sundquist, E.T., Broecker, W.S. (Eds.), *The Carbon Cycle and Atmospheric CO<sub>2</sub>: Natural Variations Archean to Present*. AGU, Washington, DC, pp. 469–486.
- Miller, K.G., Komink, M.A., Browning, J.V., Wright, J.D., Mountian, G.S., Katz, M.E., Sugarman, P.J., Cramer, B.S., Christie-Blick, N., Pekar, S.F., 2005. The Phanerozoic record of global sea-level change. *Science* 310, 1293–1298.
- Moore, T.C., Van Andel, T.H., Sancta, C., Pisias, N., 1978. Cenozoic hiatuses in pelagic sediments. *Micropaleontology* 24, 113–138.
- Naish, T., Powell, R., Levy, R., Wilson, G., Scherer, R., Talarico, F., Krissek, L., Niessen, F., Pompilio, M., Wilson, T., Carter, L., DeConto, R., Huybers, P., McKay, R., Pollard, D., Ross, J., Winter, D., Barrett, P., Browne, G., Cody, R., Cowan, E., Crampton, J., Dunbar, G., Dunbar, N., Florindo, F., Gebhardt, C., Graham, I., Hannah, M., Hansraj, D., Harwood, D., Helling, D., Henrys, S., Hinno, L., Kuhn, G., Kyle, P., Laufer, A., Maffioli, P., Magens, D., Mandernack, K., McIntosh, W., Millan, C., Morin, R., Ohneiser, C., Paulsen, T., Persico, D., Raine, I., Reed, J., Riesselman, C., Sagnotti, L., Schmitt, D., Sjuneskog, C., Strong, P., Taviani, M., Vogel, S., Wilch, T., Williams, T., 2009. Obliquity-paced Pliocene West Antarctic ice sheet oscillations. *Nature* 458, 322–328.
- Nathan, S.A., Leckie, R.M., 2009. Early history of the Western Pacific Warm Pool during the middle to late Miocene (~13.2–5.8 Ma): role of sea-level change and implications for equatorial circulation. *Palaeogeogr. Palaeoclimatol. Palaeoecol.* 274, 140–159.
- Nisancioğlu, K.H., Raymo, M.E., Stone, P.H., 2003. Reorganization of Miocene deep water circulation in response to the shoaling of the Central American Seaway. *Paleoceanography* 18, 1006.
- Opdyke, B.N., Walker, J.C.G., 1992. Return of the coral reef hypothesis: basin to shelf partitioning of CaCO<sub>3</sub> and its effect on atmospheric CO<sub>2</sub>. *Geology* 20, 733–736.
- Opdyke, B.N., Wilkinson, B.H., 1988. Surface area control of shallow cratonic to deep marine carbonate accumulation. *Paleoceanography* 3, 685–703.
- Osborne, A.H., Newkirk, D.R., Groeneveld, J., Martin, E.E., Tiedemann, R., Frank, M., 2014. The seawater neodymium and lead isotope record of the final stages of Central American Seaway closure. *Paleoceanography* 29, 715–729.
- Pälike, H., Lyle, M., Nishi, H., Raffi, I., Ridgewell, A., Gamage, K., Klaus, A., Acton, G.D., Anderson, L., Backman, J., Baldauf, J.G., Beltran, C., Bohaty, S., Brown, P.R., Busch, W.H., Channell, J.E.T., Chun, C.O.J., Delaney, M.L., Dewang, P., Dunkley Jones, T., Edgar, K.M., Evans, H.F., Fitch, P., Foster, G.L., Gussone, N., Hasegawa, H., Hathorne, E.C., Hayashi, H., Herrle, J.O., Holbourn, A., Hovan, S.A., Hyoeng, K., Iijima, K., Ito, T., Kamikuri, S.-I., Kimoto, K., Kurada, J., Leon-Rodriguez, L., Malinverno, A., Moore, T.C., Murphy, B., Murphy, D.P., Nakamura, H., Ogane, K., Ohneiser, C., Richter, C., Robinson, R.S., Rohling, E.J., Romero, O.E., Sawada, K., Scher, H.D., Schneider, L., Sluijs, A., Takata, H., Tian, J., Tsujimoto, A., Wade, B.S., Westerhold, T., Wilkins, R.H., Williams, T., Wilson, P.A., Yamamoto, Y., Yamamoto, S., Yamazaki, T., Zeebee, R.E., 2012. A Cenozoic record of the equatorial Pacific carbonate compensation depth. *Nature* 488, 609–614.
- Peters, S.E., 2006. Macrostratigraphy of North America. *J. Geol.* 114, 391–412.
- Peters, S.E., Kelly, D.C., Fraass, A.J., 2013. Oceanographic controls on the diversity and extinction of planktonic foraminifera. *Nature* 493, 398–401.
- Peters, S.E., Husson, J.M., Czaplewski, J., 2018. Macrostrat: a platform for geological data integration and deep-time earth crust research. *Geochem. Geophys. Geosyst.* 19 (4), 1393–1409.
- Pillans, B., Gibbard, P., 2012. The Quaternary Period.
- Poore, H.R., Samworth, R., White, N.J., Jones, S.M., McCave, I.N., 2006. Noogene overflow of Northern Component Water at the Greenland-Scotland Ridge. *Geochem. Geophys. Geosyst.* 7, Q06010.
- Quade, J., Cerling, T.E., Bowman, J.R., 1989. Systematic variations in the carbon and oxygen isotopic composition of pedogenic carbonate along elevation transects in the southern Great Basin, United States. *Geol. Soc. Am. Bull.* 101, 464–475.
- R Core Team, 2015. R: A Language and Environment for Statistical Computing. R Foundation for Statistical Computing, Vienna, Austria.
- Raymo, M.E., Ruddiman, W.F., Froelich, P.N., 1988. Influence of late Cenozoic mountain

- building on ocean geochemical cycles. *Geology* 16, 649–653.
- Roth, J.M., Droxler, A.W., Kameo, K., 2000. The Caribbean carbonate crash at the middle to late Miocene transition: linkage to the establishment of the modern global ocean conveyor. In: Leckie, R.M., Sigurdsson, H., Acton, G.D., Draper, G. (Eds.), Proceedings of the Ocean Drilling Program, Scientific Results. Ocean Drilling Program, College Station, TX, pp. 249–273.
- Schlanger, S.O., Douglas, R.G., 1974. Pelagic Ooze-Chalk-Limestone Transition and Its Implications for Marine Stratigraphy. Blackwell Scientific Publications, Oxford.
- Schnitker, D., 1980. North Atlantic oceanography as possible cause of Antarctic glaciation and eutrophication. *Nature* 284, 615–616.
- Sepulchre, P., Arsuze, T., Donnadieu, Y., Dutay, J.-C., Jamarillo, C., Bras, J.L., Martin, E., Montes, C., Waite, A.J., 2014. Consequences of shoaling of the Central American Seaway determined from modeling Nd isotopes. *Paleoceanography* 29, 176–189.
- Shackleton, N.J., Kennett, J.P., 1975. Paleotemperature history of the Cenozoic and initiation of Antarctic glaciation: oxygen and carbon isotopic analyses in DSDP sites 277, 279, and 281. In: Initial Reports of the Deep Sea Drilling Project, College Station, pp. 743–755.
- Shevenell, A., Kennett, J.P., Lea, D., 2004. Middle Miocene Southern Ocean cooling and Antarctic cyrosphere expansion. *Science* 305, 1766–1770.
- Spero, H.J., Bijma, J., Lea, D.W., Bemis, B.E., 1997. Effect of seawater carbonate concentration on foraminiferal carbon and oxygen isotopes. *Nature* 390, 497–500.
- Stap, L.B., Sluijs, A., Thomas, E., Lourens, L.J., 2009. Patterns and magnitude of deep sea carbonate dissolution during Eocene Thermal Maximum 2 and H2, Walvis Ridge, southeastern Atlantic Ocean. *Paleoceanography* 24, PA1211.
- Stap, L.B., van de Wal, R.S.W., de Boer, B., Bintanja, R., Lourens, L.J., 2017. The influence of ice sheets on temperature during the past 38 million years inferred from a one-dimensional ice sheet-climate model. *Clim. Past* 13, 1243–1257.
- Stein, R., Fahl, K., Schreck, M., Knorr, G., Niessen, F., Forwick, M., Gebhardt, C., Jensen, L., Kaminski, M., Kopf, A., Matthiessen, J., Jokat, W., Lohmann, G., 2016. Evidence for ice-free summers in the late Miocene central Arctic Ocean. *Nat. Commun.* 7, 1–13.
- Tedford, R.A., Kelly, D.C., 2004. A deep-sea record of the late Miocene carbon shift from the southern Tasman Sea. In: Exon, N.F., Kennett, J.P., Malone, M. (Eds.), The Cenozoic Southern Ocean; tectonics, sedimentation, and climate change between Australia and Antarctica. AGU, Washington D. C., pp. 273–290.
- Thomas, D.J., Via, R.K., 2007. Neogene evolution of Atlantic thermohaline circulation: perspective from Walvis Ridge, southeastern Atlantic Ocean. *Paleoceanography* 22, PA2212.
- Thunell, R., 1976. Optium indices of calcium carbonate dissolution in deep-sea sediments. *Geology* 4, 525–528.
- van Andel, T.H., 1975. Mesozoic/Cenozoic calcite compensation depth and the global distribution of calcareous sediments. *Earth Planet. Sci. Lett.* 26, 187–194.
- Via, R., Thomas, D.J., 2006. Evolution of Atlantic thermohaline circulation: Early Oligocene onset of deep-water production in the North Atlantic. *Geology* 34, 441–444.
- Vincent, E., Killingley, J.S., Berger, W.H., 1980. The magnetic epoch 6 carbon shift: a change in the ocean's  $^{13}\text{C}/^{12}\text{C}$  ratio 6.2 million years ago. *Mar. Micropaleontol.* 5, 185–203.
- Wolf-Welling, T.C.W., Cremer, M., O'Connell, S., Winkler, A., Thiede, J., 1996. Cenozoic arctic gateway paleoclimate variability: indications from changes in coarse-fraction composition. In: Thiede, J., Myhre, A.M., Firth, J.V., Johnson, G.L., Ruddiman, W.F. (Eds.), Proceedings of Ocean Drill Program, Scientific Results, College Station, pp. 515–567.
- Woodruff, F., Savin, S.M., 1989. Miocene deepwater oceanography. *Paleoceanography* 4, 87–140.
- Wright, J.D., Miller, K.G., 1993. Southern ocean influences on late Eocene to Miocene deepwater circulation. In: Kennett, J.P., Warnke, D. (Eds.), The Antarctica Paleoenvironment: A Prospective on Global Change, Part Two. AGU, Washington D.C., pp. 1–25.
- Wright, J.D., Miller, K.G., 1996. Control of North Atlantic deep water circulation by the Greenland-Scotland Ridge. *Paleoceanography* 11, 157–170.
- Wright, J.D., Miller, K.G., Fairbanks, R.G., 1991. Evolution of modern deepwater circulation: evidence from the late Miocene Southern Ocean. *Paleoceanography* 6, 275–290.
- Wright, J.D., Miller, K.G., Fairbanks, R.G., 1992. Early and middle Miocene stable isotopes: implications for deepwater circulation and climate. *Paleoceanography* 7, 357–389.
- Zachos, J.C., Kroon, D., Blum, P., 2004. Leg 208 Summary, Proceedings of the Ocean Drilling Program Initial Reports. Ocean Drilling Program, College Station, TX, pp. 112.
- Zachos, J.C., Dickens, G.R., Zeebe, R.E., 2008. An early Cenozoic perspective on greenhouse warming and carbon-cycle dynamics. *Nature* 451, 279–283.